Acta Metallurgica Sinica (English Letters) (2019) 32:1320–1328
https://doi.org/10.1007/s40195-019-00908-0

Dynamic Compressive Property of Closed-Cell Mg Alloy Composite Foams Reinforced with SiC Particles

Wen-Zhan Huang[1,2] · Hong-Jie Luo[1,2] · Yong-Liang Mu[1,2] · Jian-Rong Xu[1,2] · Ai-Chun Zhao[3]

Received: 25 October 2018 / Revised: 15 December 2018 / Published online: 24 April 2019

Abstract
The high-strain-rate mechanical response of Mg alloy/SiC_p composite foams has received increased attention in recent years due to their light weight and potential to absorb large amounts of energy during deformation. Dynamic compressive properties of closed-cell Mg alloy/SiC_p composite foams with different relative densities (0.162, 0.227 and 0.351) and different SiC_p additions (0, 4 and 8 wt%) have been investigated using Split-Hopkinson pressure bar. It is shown that peak stress and energy absorption capacity significantly increase as the relative density increases at the range of testing strain rates. Peak stress and energy absorption display strain rate dependence. The peak stress of specimens with 0 wt% and 4 wt% SiC particles additions grows with increasing strain rate. Meanwhile, the increment in the peak stress of specimens with 8 wt% addition is not significant with strain rate increasing. The increase in strain rate increases the energy absorption capacity. The suitable amount of SiC particles addition has great advantages over increasing the peak stress and energy absorption capacity at the high strain rate. The strain-rate-sensitive matrix, cell morphology, morphological defects and gas pressure have an impact on the strain-rate sensitivity of Mg alloy/SiC_p composite foams.

Keywords Mg alloy · SiC particles · Mg alloy/SiC_p composite foam · Split-Hopkinson pressure bar system (SHPB) · Dynamic compressive

1 Introduction

Foamed metallic materials have become potential materials for lightweight multifunctional applications due to their excellent physical and mechanical properties [1, 2]. Because of the cellular structure, closed-cell metal foams exhibit an excellent damping capacity, an outstanding sound and noise isolation and a great energy absorption [3, 4]. In practical applications, metal foams are usually subjected to high-strain-rate compressive loads. Therefore, it is necessary to investigate the compressive behavior of metal foams under dynamic compression.

Among different kinds of metallic foams, majority of the works have been focused on Al foams and its alloy foams [5–13]. Many researchers have investigated the mechanical properties of Al foams under high strain rate impact loading, but there exist contradictory opinions. Compressive strength of some closed-cell Al foams is strain rate dependent over varying strain rates [5–9]. Alporas (manufactured by a melt route) has been reported to exhibit a strain-rate sensitivity [8, 9], and the particulate SiC_p/Al- Si_9Mg composite foam has been found to be more sensitive to strain rate than Al and Al alloy foams [10]. On the other hand, other researchers have showed that the compressive strength of Al foams is apparently insensitive to strain rate. Kenny [11] and Wang et al. [12] have found that the strain-rate dependence of plateau stress for open-cell Al foam is negligible. Moreover, alulight (manufactured by a powder route) is insensitive to strain rate [13]. This arises mainly because of their different foam structures (cell shapes and sizes), porosities, homogeneity of cell walls and defects in the cell walls and fabrication

Available online at http://link.springer.com/journal/40195

✉ Hong-Jie Luo
neuhjluo@sina.com

[1] School of Metallurgy, Northeastern University, Shenyang 110819, China

[2] Engineering Research Center of Ministry of Education for Advanced Materials Preparation Technology, Shenyang 110819, China

[3] School of Materials Science and Engineering, Taiyuan University of Science and Technology, Taiyuan 030024, China

methods of foams. Previous studies have shown that the property of the cell wall material, the morphology of the cell and the preparation method might affect the high-strain-rate mechanical response of metal foams.

Recently, Mg and Mg alloy foams with the matrix density approximately two-thirds of aluminum show more promising for ultra-light metal structural materials and multifunctional materials [14]. A few recent investigations have been carried out on the compressive properties of Mg and Mg alloy foams [15–17] at low loading rates. However, there is a scarcity of studies focusing on the dynamic behavior of Mg alloy foams [18, 19]. Limited work is found about the effect of relative densities and SiC particles on the dynamic mechanical behavior of closed-cell Mg alloy/SiC_p composite foams. Therefore, further investigations are needed to examine the combined effects of strain rates, relative densities and SiC particles on the dynamic mechanical properties of Mg alloy/SiC_p composite foams, i.e., peak stress and energy absorption capacity.

The aim of the study reported here is to investigate the strain rate sensitivities of Mg alloy/SiC_p composite foams and the effects of relative densities and mass fraction of SiC particle on the dynamic compressive property. To achieve this goal, closed-cell Mg alloy/SiC_p composite foams with uniform cell distribution and small size diameter were fabricated using $MgCO_3$ as the foaming agent and SiC_p as the stabilizing agent. The Split-Hopkinson pressure bar (SHPB) technique was applied to measure the dynamic compressive behavior. After evaluation on the dynamic compressive behavior, mechanisms for the effects are discussed to be beneficial to the applications of Mg alloy/SiC_p composite foams.

2 Experimental

2.1 Materials and Specimens

Closed-cell Mg alloy/SiC_p composite foams were fabricated by the melt foaming process. After Mg–Al–Ca alloy (12 wt% Al, 3 wt% Ca) was melted, the SiC_p stabilizing agent (80 μm) was added into the melt at 580 °C, with a stirring rate of 2000 rpm for 300 s. Then, the $MgCO_3$ (100 μm) foaming agent mixed with Al_2O_3 particles (100 μm) at a mass ratio of 1:1, as an assistant dispersive agent, was added into the melt together at 580 °C, at the stirring rate of 1500 rpm for a certain time limit. The melt was put in a furnace at 620 °C for 180 s. The Mg alloy/SiC_p composite foams were obtained after the melt was taken out and cooled to room temperature. When using different fabrication parameters, such as the foaming agent content and stirring time for adding the foaming agent, the Mg alloy/SiC_p composite foams with density in a range of 0.20-0.78 g/cm^3 were generated. The effect of fabrication parameters on preparation of the composite foams has been discussed in another paper [20].

2.2 Structure Characterization

The composite foams were cut into Ø 10 mm × 8 mm by an electric discharge machining method. The specimen's density was determined through its mass and physical dimensions. Its relative density (RD) is defined as the value which is the density of composite foams divided by the density of Mg alloy matrix. The equation is given as follows:

$$\mathrm{RD} = \frac{\rho}{\rho_s}, \tag{1}$$

where ρ and ρ_s are the densities of the composite foams and the cell wall material, respectively.

The average diameter of cells was measured based on counting 600 cells according to Image-Pro Plus software. The microstructural features in composite foam were observed by scanning electron microscopy (SEM) on a microscope (Ultra Plus, Zeiss, Germany) equipped with an energy-dispersive X-ray spectroscopy (EDS) apparatus (X-Max, Oxford Instruments, England).

2.3 Mechanical Testing

Cylindrical specimens of the diameter $D = 10$ mm and length $l = 8$ mm were machined from the Mg alloy/SiC_p composite foam for high-strain-rate compression tests. All the specimens were lubricated to further minimize the interfacial friction. High-strain-rate compression tests were performed on Split-Hopkinson pressure bar system (SHPB) at strain rates ranging from 700 to 2500 s^{-1}.

The SHPB is made of solid cylindrical aluminum bars with the diameter of 12.5 mm. The lengths of striker, incident and transmitted bars are 200 mm, 900 mm and 900 mm, respectively. A schematic graph of the typical SHPB system can be found in Refs. [21, 22]. The specimen is sandwiched between the end of incident bar and the front of transmitted bar. The strain gauges mounted at the bars measure the strain waves in these bars, from which the resisting force and deformation rate of the specimen can be calculated under the assumption of uniaxial elastic stress wave propagation [19, 21–24].

3 Results and Discussion

3.1 Morphology Observation

Figure 1 shows the macrostructure and microstructure of closed-cell Mg alloy/SiC_p composite foams with 4 wt% SiC_p

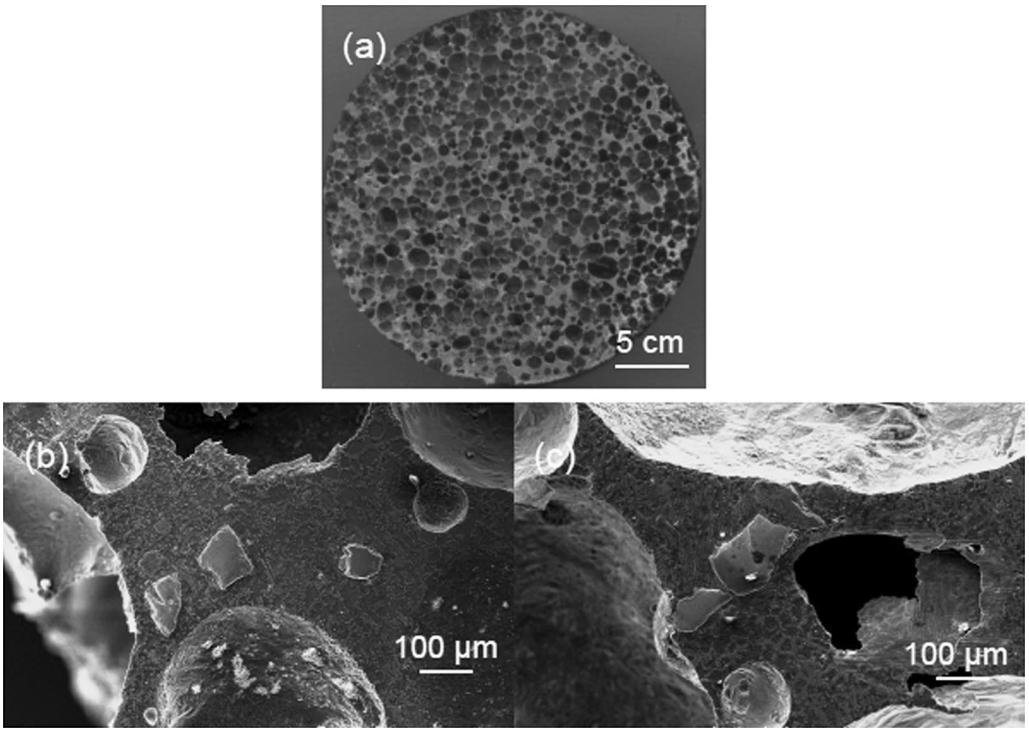

Fig. 1 Macrostructure and microstructure of closed-cell Mg alloy/SiC_p composite foams with 4 wt% SiC_p: **a** the present closed-cell foam with a relative density of 0.227, **b**, **c** distribution of SiC_p in the cell wall of foams

addition. A typical foam structure is shown in Fig. 1a. Note that the density was controlled by the processing parameters during the direct foaming process. The average diameter of cells was measured to be ~0.8 mm according to the Image-Pro Plus software. As shown in Fig. 1b, c, the uniform distribution and non-agglomeration of SiC particle in the cell wall indicate the good wettability at the SiC_p-Mg alloy melt interface, and the interface is distinct. Furthermore, heterogeneities and morphological defects such as uneven cell-wall thickness and fractured/missing cell walls are observed in the cell structure.

3.2 Effect of Relative Densities on Dynamic Compressive Response

Figure 2a–c shows engineering stress–strain plots under dynamic compression at different strain rates and relative densities. It is observed that compressive stresses at any fixed relative density increase with the strain rate. The Mg alloy/SiC_p composite foams with different relative densities (RD = 0.162, 0.227 and 0.351) exhibit an increase in peak stresses with strain rate up to 2500 s^{-1}. A critical strain rate is not observed. The critical strain rate means that the peak stress does not gain beyond this strain rate. Overall, higher increment in peak stress is observed for higher relative densities as the strain rate increases. This shows an agreement with the reported results of the Al alloy foam [22], which is a higher density foam that exhibits a significant increase in compressive stress under dynamic compression.

In this study, peak stress (σ_{Peak}) is also termed as the elastic collapse stress (σ_{el}). Figure 3 shows the variation of peak stress as a function of strain rates at different relative densities. When the strain rates are 800 s^{-1}, 800 s^{-1} and 700 s^{-1}, it is found that the peak stress of specimens is around 5.7, 12.1 and 28.3 MPa corresponding to the relative densities of 0.162, 0.227 and 0.351, respectively. Meanwhile, the peak stress of specimens is around 9.3, 19.9 and 48.7 MPa when the strain rates are 2500 s^{-1}, 2500 s^{-1} and 2100 s^{-1}, respectively. It is noted that peak stress of specimen with relative density of 0.351 increases the most. The peak stress of specimen with relative density of 0.351 is enhanced by 20.4 MPa as the strain rate increases from 700 to 2100 s^{-1}. This may be attributable to the additional effect of the gas pressure in the closed cell as described in other studies [10, 21]. In the lower-density Mg alloy/SiC_p composite foam specimens, more cell walls are thin and easy to be "blown out" at higher strain levels, which allow the gas to escape. As densities of Mg alloy/SiC_p composite foam specimens increase, the cell walls become stout and restrict the escape of gas. Thus, the gas pressure may contribute more to the strain-rate sensitivity of high relative density Mg alloy/SiC_p

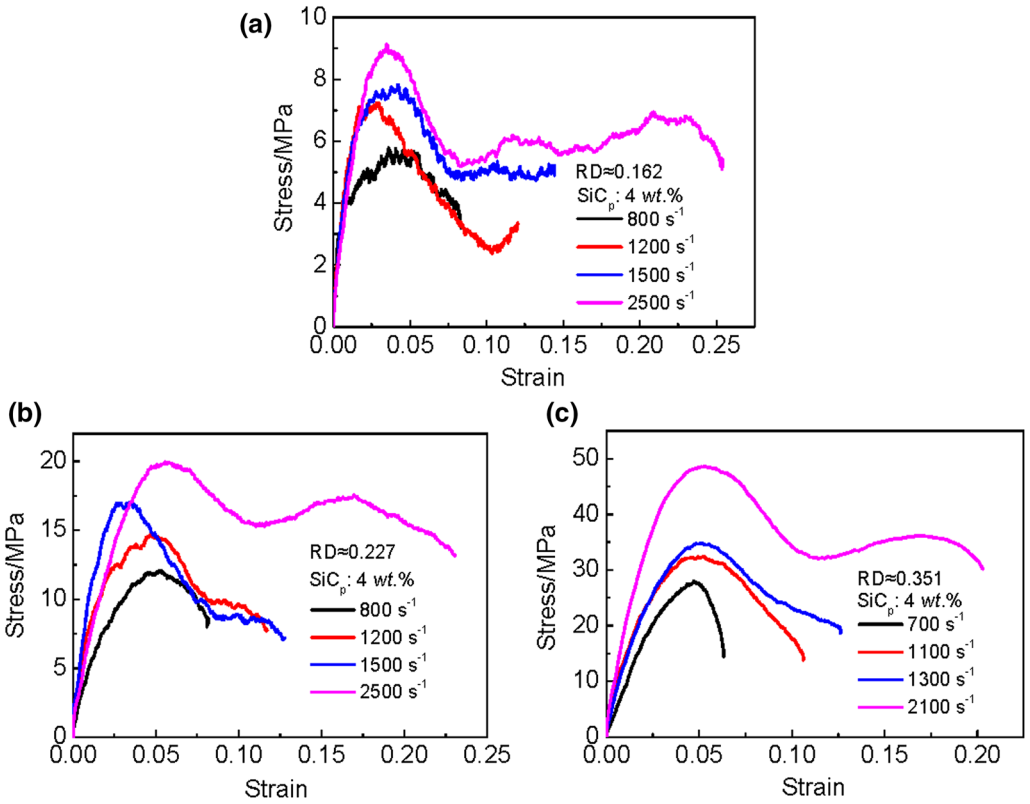

Fig. 2 Dynamic compressive stress–strain response of Mg alloy/SiC_p composite foam with different relative densities: **a** 0.162, **b** 0.227, **c** 0.351

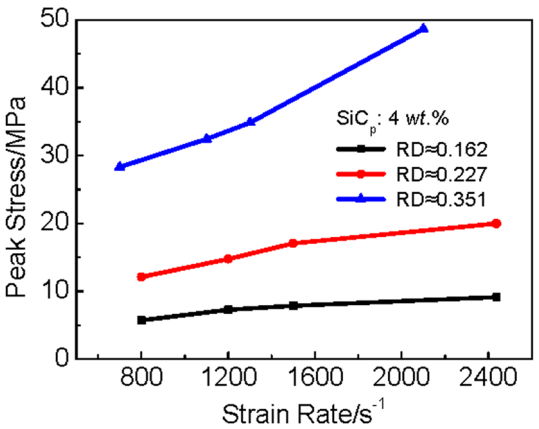

Fig. 3 Peak stress against strain rates at different relative densities

composite foams than that of low relative density Mg alloy/SiC_p composite foams.

Wang et al. [5] investigated the dynamic behaviors of aluminum foam subjected to impacting loading at temperatures ranging from 298 to 773 k. The results illustrated that strain rate effect at elevated temperature was more sensitive than that at room temperature. The deformation of aluminum foam under dynamic loading mainly resulted from the plastic bending of the cell wall at elevated temperatures, but there existed more buckling, tearing and debris profiles at room temperatures. The deformation of Mg alloy/SiC_p composite foams in this study under dynamic loading is similar to that of Al foam at room temperatures. Dannemann et al. [6] tested the dynamic compression behavior of Alporas (a closed-cell aluminum) at strain rate ranging from 400 to 2500 s^{-1}. A strain rate effect was verified for Alporas. The strain-rate effect is attributed to gas pressure and the kinetics of gas flow through the cell structure and was more significant for a high-density Alporas foam, which is consistent with the results of this paper. Zhao et al. [7] studied the impact response of Al foams made from two different manufacturing processes (IFAM and Cymat) at speed of 10 m/s. For the IFAM aluminum foam, a rate sensitivity has been observed and the deforming mode is successive folding; for the Cymat foam, no rate sensitivity is observed and the deforming mode is cell wall fracture, which provides support for the fact that the micro-inertial effect in the successive folding process is an important factor for the rate sensitivity of Al foam. However, Deshpande and Fleck [13] consider that the micro-inertial effect plays little role in enhancing the strength of metallic foam due to the bending deformation mode attributed to the large number of imperfections in

metallic foam. Meanwhile, The Mg alloy/SiC_p composite foams is brittle. The deformation under dynamic loading mainly results from buckling, tearing and debris profiles of cell wall. Therefore, the micro-inertia effect thus has a negligible effect on the rate sensitivity of Mg alloy/SiC_p composite foams.

In the compressive test, the needed energy of any foam specimen up to the specific strain is defined as the energy absorption capacity [22]. Under compressive tests, energy absorption (E) is given as the area under stress–strain curve from 0 to a specific strain ε_i and calculated by the following expression:

$$E = \int_0^{\varepsilon_i} \sigma(\varepsilon)\mathrm{d}\varepsilon, \tag{2}$$

where σ (ε) is the stress under the strain ε and ε_i is the selected strain. According to Eq. 2, energy absorption capacity of Mg alloy/SiC_p composite foams has been evaluated for different strain rates and relative densities. Figure 4 shows the energy absorption capacity of Mg alloy/SiC_p composite foams at the strain of 8% with strain rate ranging from 700 to 2500 s^{-1} for different relative densities. It can be found that the energy absorption capacity is strongly influenced by strain rate. When the strain rate is ranging from 700 to 2500 s^{-1}, the increment in the energy absorption capacity is higher as the relative density increases. At the testing strain rate range, the energy absorption capacity of specimen with relative density of 0.351 increases the most as the strain rate increases. For the specimen with relative density of 0.351, the energy absorption capacity increases from 1.21 MJ/m^3 at a strain rate of 700 s^{-1} to 3.08 MJ/m^3 at 2100 s^{-1}.

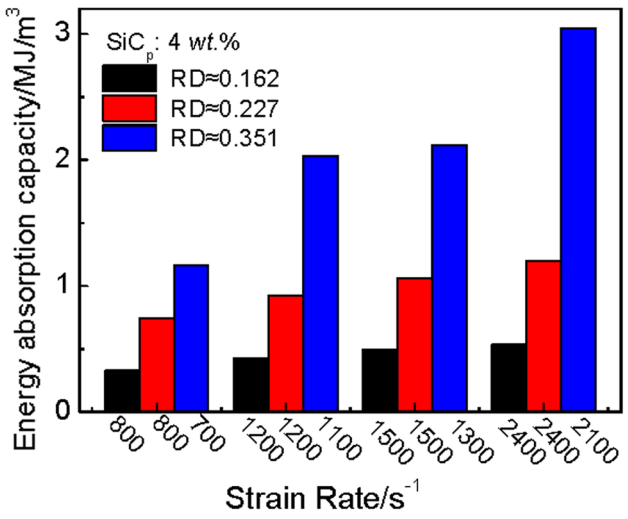

Fig. 4 Energy absorption capacity of Mg alloy/SiC_p composite foams versus strain rates with the relative densities of 0.162, 0.227 and 0.351, respectively

3.3 Effect of SiC_p on Dynamic Compressive Response

The effect of the different SiC particles additions on dynamic mechanical property of Mg alloy/SiC_p composite foams with the relative density of ~0.18 in the strain rate range 800–2500 s^{-1} is shown in Fig. 5. In Fig. 5a, b, the peak stress increases with the increase in strain rate. The peak stress is sensitive to the strain rate when the SiC particles addition is 0 wt% and 4 wt%. Compared with specimens with 0 wt% SiC particles addition, specimens with 4 wt% SiC particles addition have apparent high peak stress at the same strain rate. It proves that suitable amount of SiC particle addition has great advantages for increasing the peak stress at the high strain rate. It can be interpreted that the peak stress of Mg matrix alloy composites reinforced by SiC particle is higher than that of Mg matrix alloy due to the strengthening effect of SiC particles. It has been discussed in detail in another article [25]. Meanwhile, the additional effect of the gas pressure in the closed cell [10, 21] of the specimens with 4 wt% SiC particles addition plays a greater role than that of the specimens with 0 wt% SiC particles addition. The cell wall with 4 wt% SiC particles addition is hard to be "blown out." On the contrary, it is worth noting that the peak stress does not show a significant increasing trend with strain rate increasing in Fig. 5c. The peak stress of specimens with 8 wt% SiC particles is insensitive to the strain rate. For the limited thickness of cell wall, increasing SiC_p content has a limited strengthening effect. On the contrary, the greater the mass fraction of SiC particles is, the more brittle the composite foams are. In Mg alloy/SiC_p composite foam specimens with 8 wt% SiC_p addition, more cells are too brittle and easy to be "blown out" at higher strain levels. It allows the gas to escape and weakens the additional effect of the gas pressure in the closed cell. Thus, the increment in the peak stress of specimens with 8 wt% SiC_p addition is not evident with increasing strain rate.

It is shown that the peak stress of specimens with different SiC_p additions changes with the strain rate increasing in Fig. 6. It is worth noting that peak stress of specimens with 0 wt% and 4 wt% SiC_p additions increases with the increase in strain rate; the peak stress of specimens with 8 wt% SiC_p addition does not show a significant increasing trend with increasing strain rate. The peak stress of specimens with 0 wt%, 4 wt% and 8 wt% SiC_p additions is enhanced by 2.94 MPa, 5.19 MPa and 0.63 MPa as the strain rate increased from 800 to 2500 s^{-1}. The increment in specimens with 0 wt% and 4 wt% SiC particles additions is an order of magnitude higher than that of specimens with 8 wt% SiC_p addition. It is obvious that the increment in the peak stress of specimens with 4 wt% SiC particles addition is higher than that of specimens with 0 wt% SiC particles addition with strain rate increasing. It can be predicted that

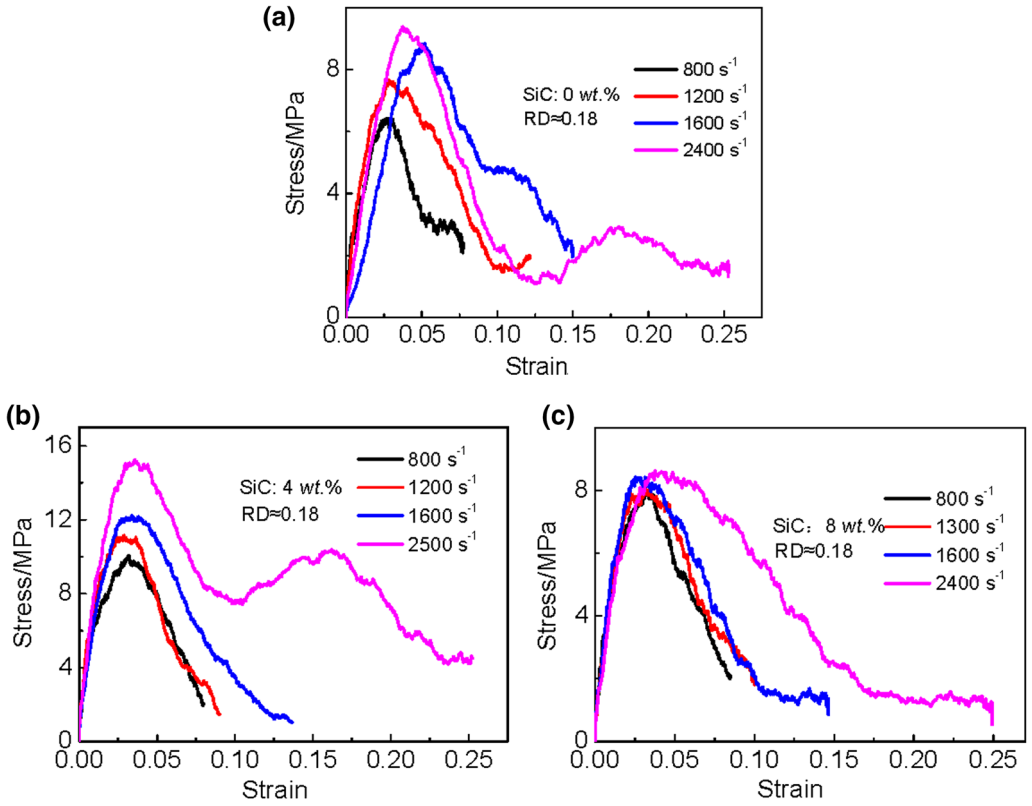

Fig. 5 Dynamic compressive stress–strain response of Mg alloy/SiC_p composite foam with different SiC_p additions: **a** 0 wt%, **b** 4 wt%, **c** 8 wt%

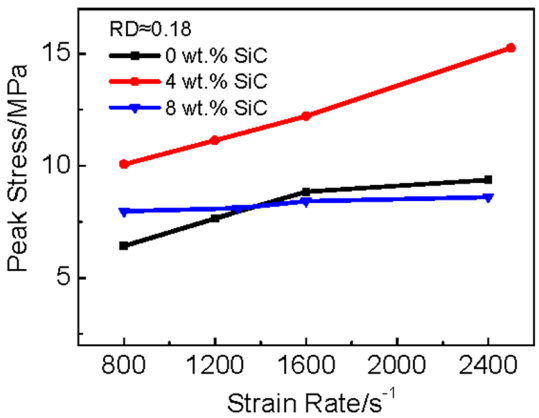

Fig. 6 Variation in the peak stress of specimens with different SiC_p additions with increasing strain rates

suitable SiC_p addition in the Mg alloy/SiC_p composite foams increases the strain rate sensitivity of specimens.

Yu et al. [10] studied the dynamic compressive behaviors of $SiC_p/AlSi_9Mg$ composite foams at the strain rate ranging from 600 to 1600 s^{-1}. The experimental results showed that $SiC_p/AlSi_9Mg$ composite foams had a strain rate effect and was more sensitive to the strain rate than Al and Al alloy foams. The yield stress of the composite foams with different SiC particles addition at high strain rate increased with the increase in the volume fraction of SiC particles. SiC_p particles played a strengthening effect in $SiC_p/AlSi_9Mg$ composite foams. Meanwhile, SiC_p particles made the composite foams more brittle because the addition of SiC particles leads to more interface. The mechanism of SiC particles in dynamic compression process of $SiC_p/AlSi_9Mg$ composite foams is the same as that of Mg alloy/SiC_p composite foams. However, the peak stress of specimens with 8 wt% SiC particles is insensitive to the strain rate in this study, which is not observed in the other studies [10, 25]. This may be caused by that the ceramic particle content in the other studies still does not exceed the critical value.

Figure 7 shows the energy absorption capacity of Mg alloy/SiC_p composite foams with different SiC_p additions at the strain of 8% with strain rate ranging from 800 to 2500 s^{-1}. It can be found that the energy absorption capacity increases with strain rate increasing. When the strain rate is ranging from 800 to 2500 s^{-1}, the increment in the energy absorption capacity of specimens is 0.215, 0.382 and 0.131 MJ/m^3 corresponding to the SiC_p addition of 0, 4 and 8 wt%. At the testing strain rate range, the energy absorption capacity of specimen with 4 wt% SiC_p addition grows the most as the strain rate increases. Compared with the specimens with different relative densities, the increment in the

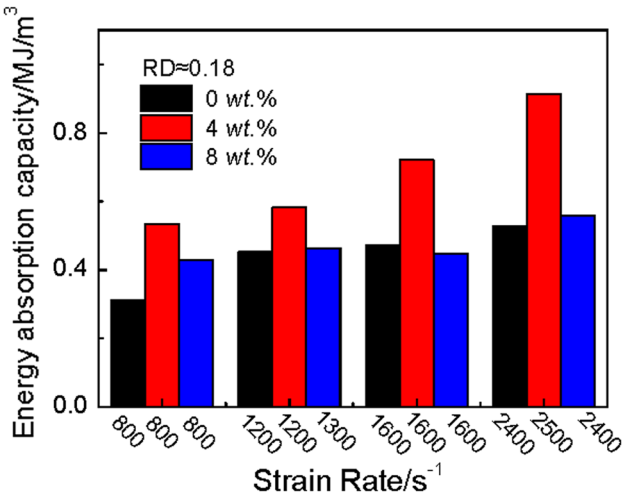

Fig. 7 Energy absorption capacity of Mg alloy/SiC_p composite foams versus strain rates with different SiC_p additions

energy absorption capacity of the specimens with different SiC_p additions is small.

Figure 8 shows the compressive final morphologies of Mg alloy/SiC_p composite foams with 8 wt% SiC_p with strain rate ranging from 800 to 2400 s^{-1}. The composite foams produce many crushed fragments at strain rate of 2400 s^{-1}. When the strain rate increases from 800 to 2400 s^{-1}, more and more fragments are observed, which indicates that the composite foams display brittle fracture behavior. The brittleness of the Mg alloy/SiC_p composite foams induces the stress oscillations during compression, which is in agreement with the observations in Figs. 2 and 5.

Figure 9 demonstrates the SEM image of the fracture surfaces in the fragments of the Mg alloy/SiC_p composite foams after the dynamic compression. The cracks in the weak link and defects in the cells are shown in Fig. 9a. Meanwhile, cracks occur at multiple locations along the cell wall resulting in the fracture and collapse of the cell wall. It is shown that fracture and collapse occur on the cell wall resulting in producing crushed fragments in Fig. 9b, which is in agreement with the observations in Fig. 8. In addition, the cell edge is more prone to fracture and collapse (shown from Fig. 9c, d) than the plateau border. The fracture and collapse occur along the cell edge, while plateau border is still relatively intact.

3.4 Mechanisms of the Strain-Rate Sensitivity of Mg Alloy Foam

The exact mechanisms of the strain-rate sensitivity of Mg alloy/SiC_p composite foam have not been established. The most prevalent explanation is that metal foam with a rate-sensitive matrix is strain rate sensitive [26]. In addition, cell morphology and morphological defects also play a crucial rule in the rate sensitivity of metal foam [8, 19, 26]. The strain rate dependence of mechanical strength for Mg and Mg alloys has been demonstrated [27–29]. Thus, the strain-rate-sensitive matrix contributes to the increase in the peak stress of Mg alloy/SiC_p composite foams at high strain rates. For the closed-cell Mg alloy/SiC_p composite foam, pressurization of the gas within the cells and movement of the gas through the cells as cell walls rupture, i.e., the gas pressure effect, also lead to strain rate dependency of Mg alloy/SiC_p composite foam. Morphological defects such as microcracks and mutilated cells are inevitable in the specimen as well. The defects allow the gas to escape. As discussed previously, it is clear that the strain-rate sensitivity of Mg alloy/SiC_p composite foam also can be attributed to the strain-rate-sensitive matrix. Moreover, cell morphology and morphological defects also play a crucial rule in the strain rate sensitivity of Mg alloy/SiC_p composite foam. Based on the discussions above, the stress of Mg alloy/SiC_p composite foam at high strain rates is mainly composed of three parts. An equation on stress at high strain rates is given by

$$\sigma = \sigma_{Mg} + \sigma_{CS} + \sigma_{GP}, \tag{3}$$

where σ is the stress of Mg alloy/SiC_p composite foam at high strain rates, σ_{Mg} is the stress influenced by the Mg alloy/SiC_p matrix, σ_{CS} is the stress affected by cell structure and σ_{GP} is the stress impacted by the gas pressure. The major

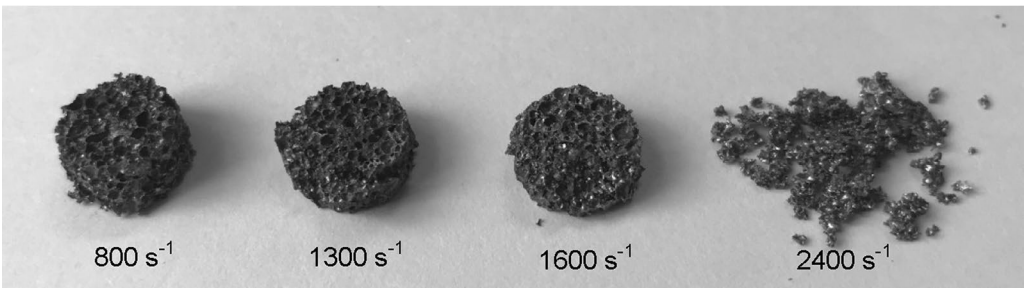

Fig. 8 Dynamic compressive final morphologies of Mg alloy/SiC_p composite foams with 8 wt% SiC_p with different strain rates

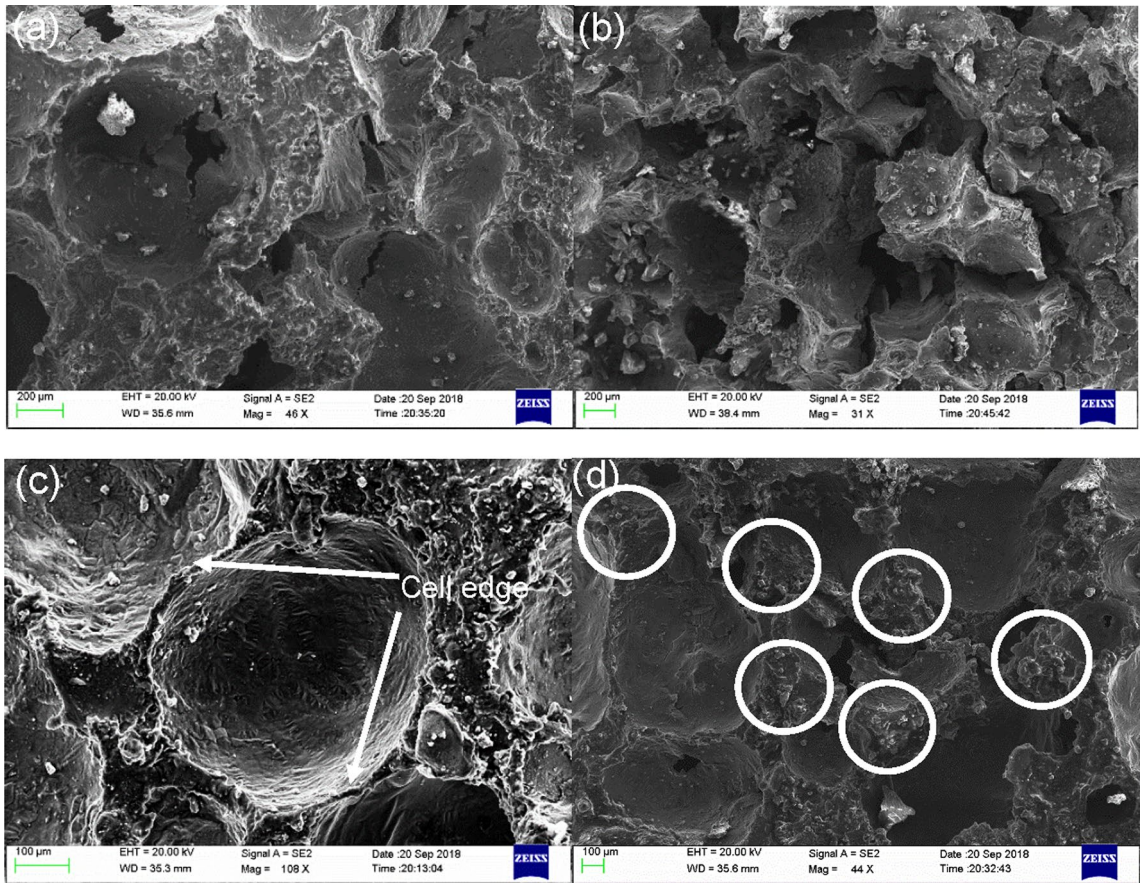

Fig. 9 SEM image of the fracture surfaces in the fragments of the Mg alloy/SiC_p composite foams after the dynamic compression: **a** cracks in the cell walls, **b**–**d** the fracture and collapse of the cell wall. (Note: arrows indicate the cell edge, the boxed-in area of the figure (**d**) is plateau border)

effect among them is different at variation of high strain rates, relative densities and SiC_p addition.

4 Conclusions

Dynamic compressive mechanical properties of closed-cell Mg alloy/SiC_p composite foams have been investigated under dynamic loading with different relative densities (0.162, 0.227 and 0.351) and different SiC_p additions (0, 4 and 8 wt%). Split-Hopkinson pressure bar was used to study the dynamic compression behavior. The conclusions were drawn as follows.

1. For similar strain rates, peak stress and energy absorption capacity are higher for higher relative densities. Specimen with relative density of 0.351 has the highest peak stress and energy absorption capacity.
2. For all densities, the peak stress and energy absorption capacity increase with the strain rate. Peak stress and energy absorption display strain rate dependence. At the testing strain rate ranges, the higher the relative densities are, the higher the increment in peak stress and energy absorption capacity will be, when the strain rate increases. Both peak stress and energy absorption capacity of specimen with relative density of 0.351 increase the most as the strain rate increases.
3. The peak stress of specimens with 0 wt% and 4 wt% SiC particles additions increases with strain rate increasing. Meanwhile, the increment in the peak stress of specimens with 8 wt% addition is not evident with increasing strain rate. The energy absorption capacity increases with strain rate increasing. At the testing strain rate ranges, the increment in the energy absorption capacity of specimen with 4 wt% SiC_p addition is the most as the strain rate increases. The suitable amount of SiC particles addition has a great advantage for increasing the peak stress and energy absorption capacity at the high strain rate.

Acknowledgements This work was financially supported by National Natural Science Foundation of China (Nos. 51874093, 51174060 and 51301109) and Fundamental Research Funds for the Central Universities (No. N162410002-2-10).

References

[1] L.J. Gibson, M.F. Ashby, *Cellular Solids: Structures and Properties* (Cambridge University Press, Cambridge, 1997)
[2] H. Kanahashi, T. Mukai, Y. Yamada, K. Shimojima, M. Mabuchi, T. Aizawa, K. Higashi, Mater. Sci. Eng. A **308**, 283 (2001)
[3] X.H. Liu, H.Y. Huang, J.X. Xie, Int. J. Min. Met. Mater. **21**, 687 (2014)
[4] D.R. Tian, Y.H. Pang, L. Yu, L. Sun, Int. J. Min. Met. Mater. **23**, 793 (2016)
[5] P.F. Wang, S.L. Xu, Z.B. Li, J.L. Yang, H. Zheng, S.S. Hu, Mater. Sci. Eng. A **599**, 174 (2014)
[6] K.A. Dannemann, J. Lankford, Mater. Sci. Eng. A **29**, 157 (2000)
[7] H. Zhao, I. Elnasri, S. Abdennadher, Int. J. Mech. Sci. **47**, 757 (2005)
[8] T. Mukai, H. Kanahashi, T. Miyoshi, M. Mabuchi, T.G. Nieh, K. Higashi, Scr. Mater. **40**, 921 (1999)
[9] S. Ramachandra, P. Sudheer Kumar, U. Ramamurty, Scr. Mater. **49**, 741 (2003)
[10] S.R. Yu, Y.R. Luo, J.A. Liu, Mater. Sci. Eng. A **487**, 394 (2008)
[11] L.D. Kenny, Mater. Sci. Forum **217**, 1883 (1996)
[12] Z.H. Wang, H.W. Ma, L.M. Zhao, G.T. Yang, Scr. Mater. **54**, 83 (2006)
[13] V.S. Deshpande, N.A. Fleck, Int. J. Impact Eng. **24**, 277 (2000)
[14] W.Z. Huang, H.J. Luo, Y.L. Mu, H. Lin, H. Du, Int. J. Min. Met. Mater. **24**, 701 (2017)
[15] D.H. Yang, S.R. Yang, H. Wang, A.B. Ma, J.H. Jiang, J.Q. Chen, D.L. Wang, Mater. Sci. Eng. A **527**, 5405 (2010)
[16] Z.G. Xu, J.W. Fu, T.J. Luo, Y.S. Yang, Mater. Des. **34**, 40 (2012)
[17] Y. Yamada, K. Shimojima, Y. Sakaguchi, M. Mabuchi, M. Nakamura, T. Asahina, T. Mukai, H. Kanahashi, K. Higashi, Mater. Sci. Eng. A **28**, 225 (2000)
[18] T. Mukai, H. Kanahashi, Y. Yamada, K. Shimojima, M. Mabuchi, T.G. Nieh, K. Higashi, Scr. Mater. **41**, 365 (1999)
[19] P.F. Li, N.V. Nguyen, H. Hao, Mater. Des. **89**, 636 (2016)
[20] H.J. Luo, L. Zhang, Z.G. Xu, Y.S. Yang, Mater. Sci. Forum **749**, 356 (2012)
[21] T. Mukai, T. Miyoshi, S. Nakano, H. Somekawa, Scr. Mater. **54**, 533 (2006)
[22] A. Aldoshan, S. Khanna, Mater. Sci. Eng. A **689**, 17 (2017)
[23] P. Li, N. Petrinic, C.R. Siviour, R. Froud, J.M. Reed, Mater. Sci. Eng. A **515**, 19 (2009)
[24] J.T. Fan, J. Weerheijm, L.J. Sluys, Mater. Des. **79**, 73 (2015)
[25] W.Z. Huang, H.J. Luo, H. Lin, Y.L. Mu, B. Ye, J. Mater. Eng. Perform. **25**, 1 (2016)
[26] Y.L. Mu, G.C. Yao, Z.K. Cao, H.J. Luo, G.Y. Zu, Scr. Mater. **64**, 61 (2011)
[27] H. Asgari, J.A. Szpunar, A.G. Odeshi, Mater. Des. **61**, 26 (2014)
[28] I.C. Choi, D.H. Lee, B. Ahn, K. Durst, M. Kawasaki, T.G. Langdon, J.I. Jang, Scr. Mater. **94**, 44 (2015)
[29] W.Q. Song, P. Beggs, M. Easton, Mater. Des. **30**, 642 (2009)